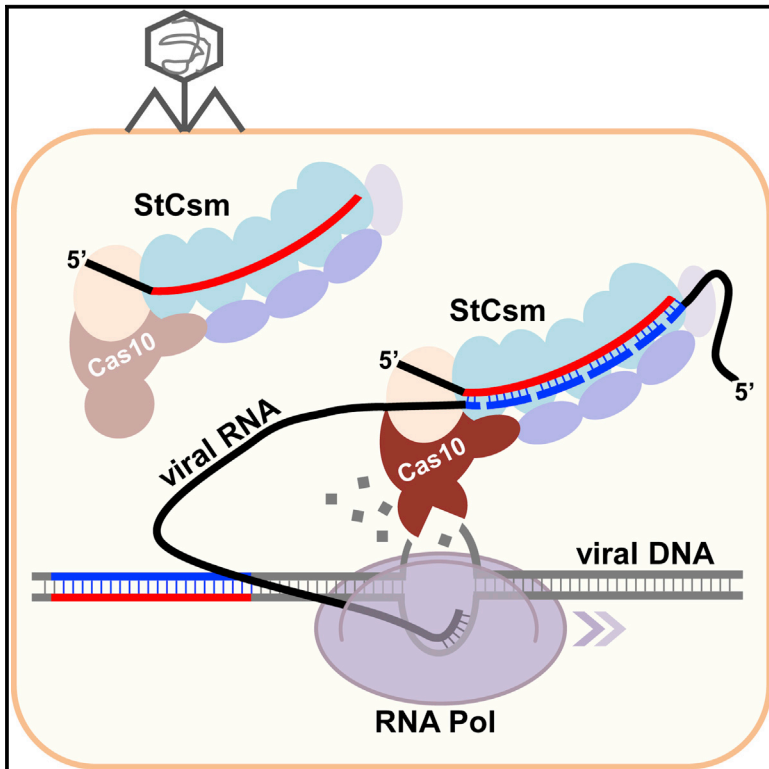


Spatiotemporal Control of Type III-A CRISPR-Cas Immunity: Coupling DNA Degradation with the Target RNA Recognition

Graphical Abstract



Authors

Migle Kazlauskienė,
Gintautas Tamulaitis, Georgij Kostiuk,
Česlovas Venclovas, Virginijus Siksnys

Correspondence

tamulaitis@ibt.lt (G.T.),
siksnys@ibt.lt (V.S.)

In Brief

Kazlauskienė et al. report a mechanism for RNA-dependent DNA degradation by a type III-A CRISPR-Cas complex. Target RNA binding activates DNA degradation whereas subsequent RNA cleavage represses DNase activity, providing a spatiotemporal control. The complementarity of the 5' handle of crRNA to the target RNA, but not DNA, protects host DNA from degradation.

Highlights

- Target RNA binding by the type III-A StCsm complex activates ssDNA degradation
- HD-domain of the Cas10 subunit is responsible for the ssDNase activity
- Fast cleavage of the target RNA by Csm3 subunit ensures temporal control of Cas10 DNase
- Base-pairing between the target RNA and the crRNA 5'-handle prevents self-targeting



Spatiotemporal Control of Type III-A CRISPR-Cas Immunity: Coupling DNA Degradation with the Target RNA Recognition

Migle Kazlauskienė,^{1,2} Gintautas Tamulaitis,^{1,2,*} Georgij Kostiuk,¹ Česlovas Venclovas,¹ and Virginijus Siksnys^{1,*}

¹Institute of Biotechnology, Vilnius University, Graiciuno 8, Vilnius 02241, Lithuania

²Co-first author

*Correspondence: tamulaitis@ibt.lt (G.T.), siksnys@ibt.lt (V.S.)

<http://dx.doi.org/10.1016/j.molcel.2016.03.024>

SUMMARY

Streptococcus thermophilus (St) type III-A CRISPR-Cas system restricts MS2 RNA phage and cuts RNA in vitro. However, the CRISPR array spacers match DNA phages, raising the question: does the St CRISPR-Cas system provide immunity by erasing phage mRNA or/and by eliminating invading DNA? We show that it does both. We find that (1) base-pairing between crRNA and target RNA activates single-stranded DNA (ssDNA) degradation by StCsm; (2) ssDNase activity is confined to the HD-domain of Cas10; (3) target RNA cleavage by the Csm3 RNase suppresses Cas10 DNase activity, ensuring temporal control of DNA degradation; and (4) base-pairing between crRNA 5'-handle and target RNA 3'-flanking sequence inhibits Cas10 ssDNase to prevent self-targeting. We propose that upon phage infection, crRNA-guided StCsm binding to the emerging transcript recruits Cas10 DNase to the actively transcribed phage DNA, resulting in degradation of both the transcript and phage DNA, but not the host DNA.

INTRODUCTION

CRISPR-Cas systems provide prokaryotes with resistance against invading genetic elements and are subdivided into five major types (I–V) that differ by nucleic acid (NA) target, number and arrangement of *cas* genes, and the composition of a silencing complex (Makarova et al., 2015). In type I and II systems, ribonucleoprotein (RNP) complexes, termed Cascade and Cas9, respectively, recognize foreign DNA through base-pairing with crRNA and trigger DNA degradation by an auxiliary Cas3 nuclease/helicase (Sinkunas et al., 2011; Westra et al., 2012) or the Cas9 protein (Gasiunas et al., 2012; Jinek et al., 2012). Despite structural differences, type I and II silencing complexes share conserved mechanistic features: they target DNA, require a protospacer adjacent motif (PAM) to discriminate between self and non-self DNA and form an R-loop as a reaction intermediate (Gasiunas et al., 2014).

Molecular mechanisms of type III CRISPR-Cas systems remain to be established. Type III systems are classified into four subtypes (III A–D) and require large RNP complexes for NA interference (Makarova et al., 2015). Cascade (type I) and Cmr (III-B) NA silencing complexes are evolutionary and structurally related (Jackson et al., 2014; Makarova et al., 2015; Mulepati et al., 2014; Osawa et al., 2015; Zhao et al., 2014); however, the NA targets and molecular mechanisms are distinct. Cascade targets exclusively DNA, whereas the Cmr complex in vivo presumably targets both RNA and DNA (Deng et al., 2013; Peng et al., 2015). Although the RNA cleavage by the Cmr complex has been already demonstrated (Benda et al., 2014; Hale et al., 2014; Ramia et al., 2014a; Staals et al., 2013; Zhang et al., 2012; Zhu and Ye, 2015), DNA cleavage activity still remains to be reconstituted in vitro.

On the other hand, genetic studies demonstrated DNA targeting for the type III-A Csm complex in *Staphylococcus epidermidis* (SeCsm) (Marraffini and Sontheimer, 2008), whereas crRNA-guided RNA cleavage has been shown in vitro (Samai et al., 2015). Transcription through the target has been required for DNA targeting in vivo (Goldberg et al., 2014). Recently, Samai et al. have shown that the transcription across the target results in the dual cleavage of the target DNA and the RNA transcript and concluded that the crRNA-guided SeCsm independently targets either RNA or single-stranded (ss) DNA through base-pairing (Samai et al., 2015). The RNA targeting triggered RNA cleavage by the Csm3 RNase subunit of the SeCsm complex. crRNA-guided DNA targeting activated DNA cleavage by the Cas10 subunit that possesses HD-nuclease and polymerase(Pol)/cyclase-like domains (Makarova et al., 2015). Samai et al. demonstrated that the DNase activity of SeCsm depends on the GGDD-motif of the Cas10 Pol-domain. This raises a question as to the role of the Cas10 HD-domain, because in the structurally and evolutionary related type I CRISPR-Cas systems, it is the HD-domain of the Cas3 nuclease/helicase that is responsible for the ssDNA degradation (Sinkunas et al., 2011; Westra et al., 2012). Furthermore, it remains unclear how independent RNase and DNase activities of the SeCsm complex are coordinated in space and time to ensure the destruction of foreign genetic elements while preventing the degradation of host DNA. Based on genetic studies it was suggested that the pairing between the crRNA 5'-handle and the 3'-flanking sequence of the target DNA prevents host DNA cleavage and contributes to discrimination between self and non-self by the type III systems (Marraffini and

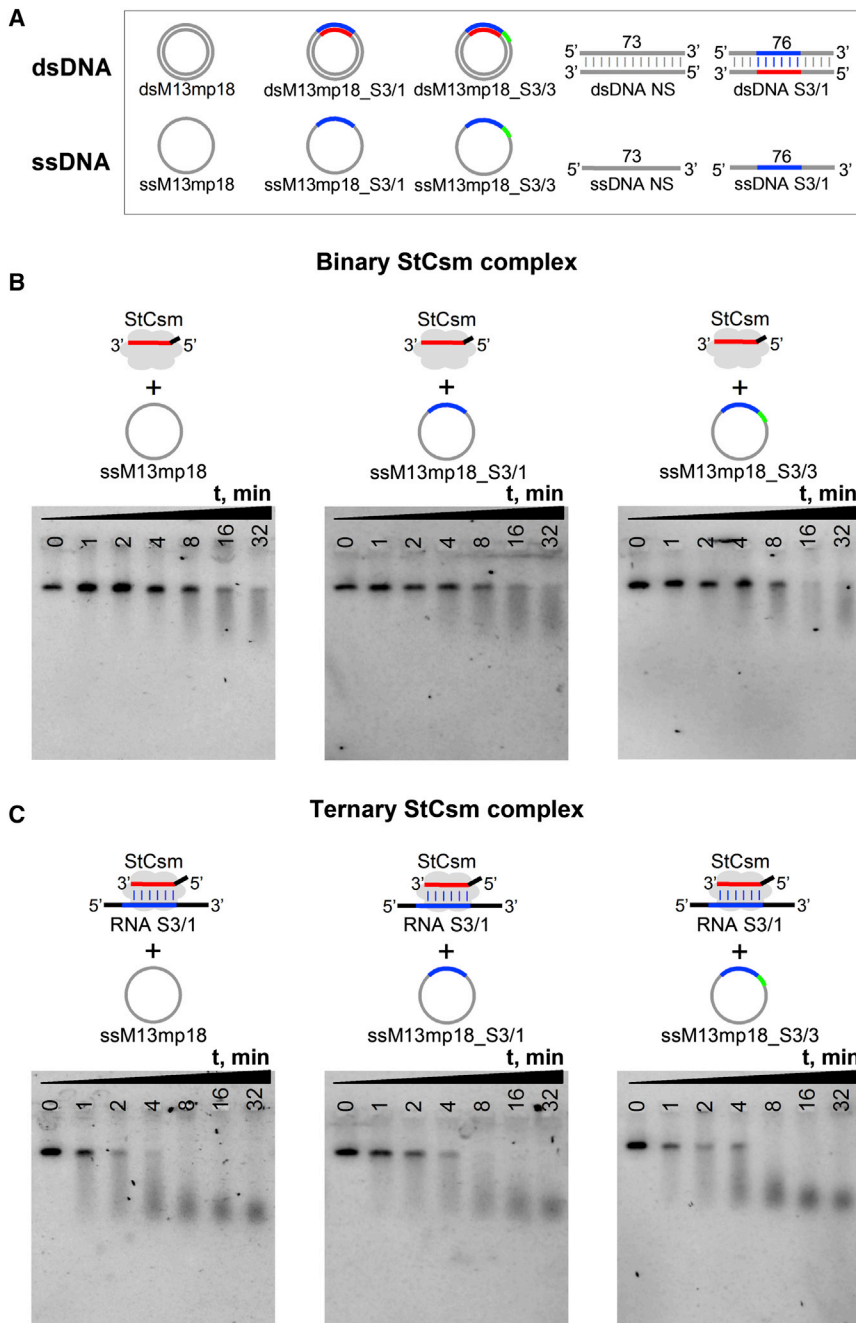


Figure 1. Closed Circular ssDNA Degradation by StCsm

(A) dsDNA and ssDNA substrates used in this study. Protospacer is blue, the complementary strand (matching spacer in crRNA) is red. 3'-flanking sequences of protospacer complementary to 5'-handle of crRNA are green.

(B and C) ssDNA cleavage by the binary (B) and ternary (C) StCsm complexes. The reactions contained 5 nM of binary or ternary StCsm and 1 nM of ssDNA. Reactions were initiated by addition of Mn^{2+} and products were analyzed on agarose gels.

DNA does not prevent DNA cleavage. Instead, we show that the base-pairing between the 5'-handle of crRNA and the target RNA 3'-flanking sequence suppresses the ssDNase activity of Cas10 and thereby ensures discrimination between self and non-self DNA. Finally, we propose a mechanism for a spatio-temporal regulation of the type III-A CRISPR-Cas immunity that ensures selective degradation of both mRNA and DNA of invading genetic elements but prevents damage to the host genome.

RESULTS

DNA Degradation by the Binary StCsm Complex

The binary StCsm complex isolated from the heterologous *E. coli* strain is composed of Csm proteins with the stoichiometry Cas10₁:Csm2₃:Csm3₅:Csm4₁:Csm5₁ and contains a 40 nucleotide (nt) crRNA consisting of an 8 nt 5'-handle and a 32 nt sequence complementary to the S3 spacer in the type III-A CRISPR array of the *S. thermophilus* DGCC8004 strain (Tamulaitis et al., 2014). To monitor DNA cleavage by the binary StCsm complex, we engineered derivatives of the M13mp18 plasmid DNA that can be isolated in either double-stranded (ds) or ss closed circular forms.

The parental M13mp18 DNA lacks the sequence complementary to the crRNA, whereas M13mp18_S3/1 and M13mp18_S3/3 variants contain the S3 protospacer sequence that is flanked by the 3'-sequence either non-complementary or complementary to the 5'-handle of crRNA (Figure 1A; Table S1). In addition, linear ssDNA or dsDNA oligonucleotides containing (76-mer) or lacking (73-mer) the S3/1 protospacer sequence (Figure 1A; Table S1) were used in the cleavage assays. Consistent with findings from previous studies, dsDNAs in linear or closed circular forms were resistant to StCsm cleavage (Figure S1). In contrast, closed circular ssDNAs were slowly

Sontheimer, 2010); however, this mechanism has yet to be confirmed.

Here we have focused on the molecular mechanism of NA interference by the *S. thermophilus* type III-A Csm (StCsm) complex, which is homologous to SeCsm (Tamulaitis et al., 2014). We show here that StCsm in vitro functions as an RNA-stimulated ssDNase that couples the target RNA binding/cleavage with ssDNA degradation. We demonstrate that HD-domain of the Cas10 subunit in the StCsm complex is responsible for the ssDNA degradation and that the complementarity between the crRNA 5'-handle and the 3'-flanking sequence of the target

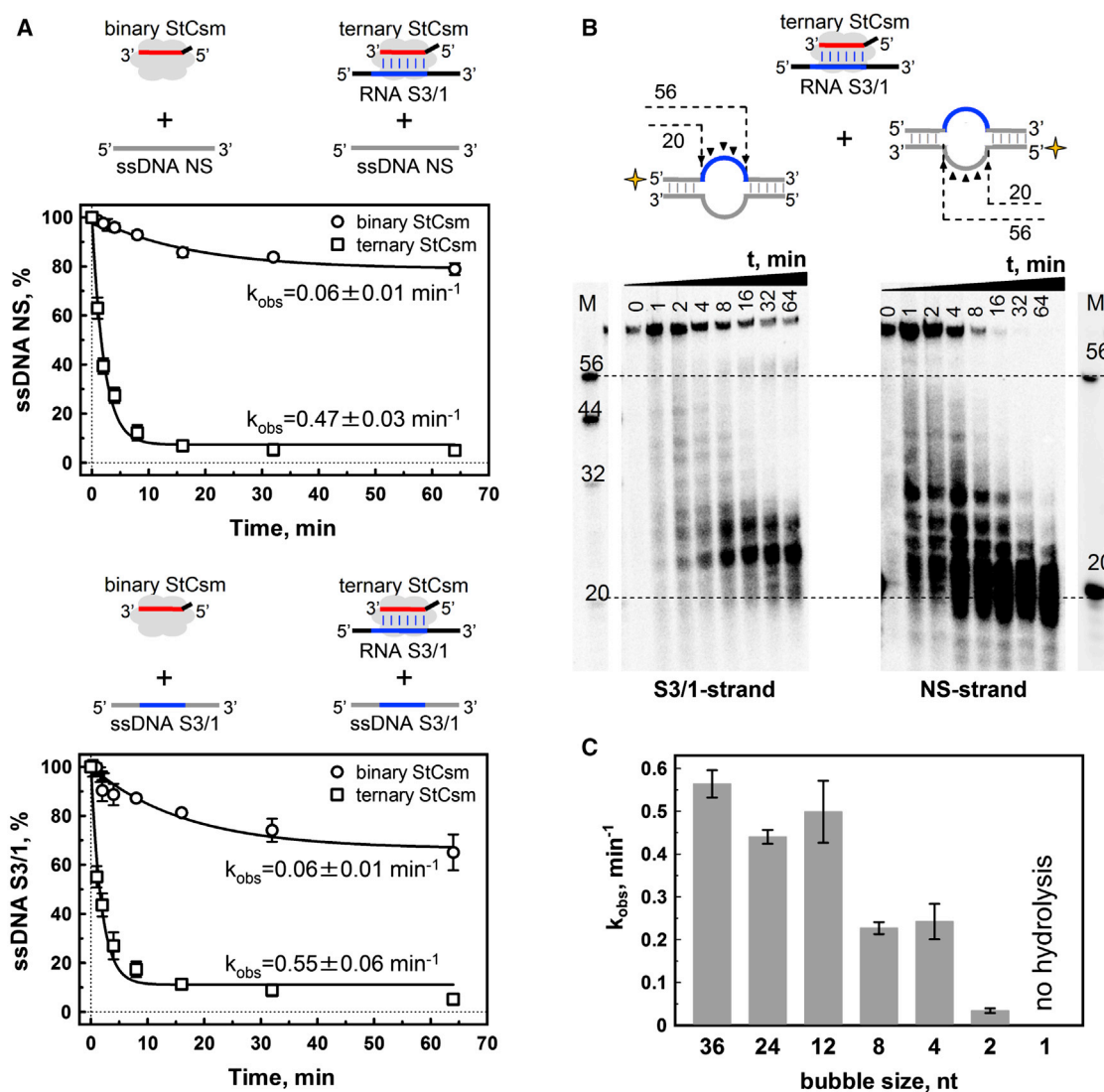


Figure 2. StCsm Reactions on Single-Stranded Oligodeoxynucleotides and DNA Bubbles

(A) Time course of oligodeoxynucleotide degradation: 4 nM of ^{32}P -labeled ssDNA S3/1 (76-mer containing the protospacer) or NS (73-mer lacking a protospacer) were incubated with 200 nM of the binary or ternary StCsm complex in a reaction buffer. Reaction was initiated by addition of 10 mM of MnCl_2 , aliquots were withdrawn at fixed time and products analyzed in PAAG gels. Rate constants were calculated by fitting single exponentials to the substrate depletion data. Cartoons above the graphs depict reaction components (see Figure 1 legend for color coding).

(B) Cleavage of bubbled DNA by the ternary StCsm complex. Ternary StCsm was incubated with DNA duplex containing 36 nt unpaired region. The S3/1-strand (top strand) contains S3 protospacer sequence, the NS-strand (bottom strand) lacks the sequence complementary to the crRNA. Cleavage reactions contained 4 nM of oligoduplex, ^{32}P -labeled either on S3/1-strand or NS-strand (indicated by a star), and 200 nM of the ternary StCsm. Cartoons above the graphs depict reaction components (see Figure 1 legend for color coding). Triangles denote cleavage positions; M, synthetic DNA markers.

(C) Rates of the NS-strand degradation by the ternary StCsm. Synthetic DNA duplexes containing unpaired regions of different length (from 36 nt to 1 nt) that produce DNA bubbles of different size or mismatches were incubated with StCsm under the reaction conditions described in (B) and reaction rates were determined as in (A).

degraded by the binary StCsm complex producing a characteristic smear in agarose gel indicative of random cleavage (Figure 1B). Notably, the cleavage patterns were nearly identical for the closed circular ssDNA lacking the protospacer sequence and ssDNAs containing the protospacer S3 flanked by the 3'-sequence either non-complementary or complementary to the crRNA 5'-handle. Linear oligodeoxynucleotides were also

slowly degraded by the binary StCsm complex with nearly the same rate ($k_{obs} \approx 0.06 \pm 0.01 \text{ min}^{-1}$) (Figure 2A), no matter whether the complementary protospacer sequence was present.

DNA Degradation by the Ternary StCsm Complex

The binary StCsm complex bound the complementary target RNA into the ternary complex (Tamulaitis et al., 2014). Samai

et al. have recently shown that transcription across the SeCsm target was absolutely required for DNA targeting (Samai et al., 2015). To probe whether the target RNA binding into the ternary complex may alter its biochemical activities, we analyzed the DNase activity of the ternary StCsm complex in the presence of Mn^{2+} ions that support DNA cleavage (Jung et al., 2015; Ramia et al., 2014b). All dsDNA variants in both closed circular and linear forms were resistant to cleavage by the ternary StCsm complex (Figure S1). In contrast, the ternary StCsm complex cleaved closed circular ssDNA substrates much faster than the binary complex, suggesting that the target RNA binding stimulates ssDNA cleavage (Figure 1C). Notably, DNA degradation rate increase manifested as a shift of smeared bands toward shorter times for the ternary StCsm complex in comparison with the binary complex (Figures 1B and 1C) and was essentially unaffected by the presence or absence of the complementary protospacer sequence (Figure 1C).

We found that Mn^{2+} , Ni^{2+} , or Co^{2+} ions supported DNA degradation by StCsm and that the metal ion chelation by EDTA inhibited the reaction (Figure S2A). On the other hand, Mg^{2+} , Ca^{2+} , or Zn^{2+} ions that were required for the RNase activity of the Csm3 subunit (Tamulaitis et al., 2014) did not support the DNase activity of StCsm. Among the metal cofactors tested, only Mn^{2+} and Ni^{2+} ions supported both RNase and ssDNase activity of the StCsm complex.

To quantitate ssDNA degradation by binary and ternary StCsm complexes, we analyzed cleavage of the 5'-radioactively labeled ssDNA oligonucleotides either containing or lacking the S3 protospacer sequence (Figure 2A; Figure S2B). We found that independently of whether the complementary protospacer sequence was present, the ssDNA oligonucleotides were degraded by the ternary StCsm complex nearly 10-fold faster than by the binary complex (Figure 2A). Taken together, cleavage data for both closed circular and linear ssDNA substrates show that binding of the target RNA into the ternary complex activates ssDNA degradation.

DNA Degradation by the Ternary StCsm-DNA Complex

Next, we tested whether the ternary complex that includes complementary DNA instead of RNA may also activate ssDNA degradation. Binary StCsm indeed bound a ssDNA S3/1 oligonucleotide into a ternary complex; however, the binding affinity was nearly 30-fold lower in comparison to the ssRNA target (Tamulaitis et al., 2014).

To test whether the pre-assembled StCsm-DNA ternary complex stimulates ssDNA degradation *in trans*, we analyzed the cleavage of ssM13mp18 DNA by the StCsm bound to the ssDNA S3/1 oligonucleotide. We found that unlike the ternary StCsm-RNA complex, the ternary StCsm-DNA complex did not activate the ssM13mp18 DNA degradation (Figure S3).

To test whether the target DNA binding by the binary StCsm complex is able to self-activate the target ssDNA degradation *in cis*, we pre-bound StCsm binary complex to the ssM13mp18 plasmids that contained the protospacer sequence complementary to the crRNA, added Mn^{2+} cofactor, and monitored ssDNA degradation in agarose gel. Because protospacer 3'-flanking sequence was shown to play a key role in the DNA interference and self- versus non-self DNA discrimination

by the SeCsm complex (Marraffini and Sontheimer, 2010), we used two ssM13mp18 variants where the 3'-protospacer flanking sequence was either complementary or non-complementary to the 5'-handle of the crRNA (Figure 1A). We found that ssM13mp18 DNA pre-bound to the StCsm complex did not trigger ssDNA degradation independently of the protospacer 3'-flanking sequence being complementary or non-complementary to the 5'-handle of crRNA (Figure 1B). Thus, the target DNA binding into the ternary StCsm complex instead of RNA did not activate ssDNA degradation.

EMSA Analysis of NA Binding by the Binary and Ternary StCsm Complexes

To further understand NA binding features of the ternary StCsm-RNA, StCsm-DNA, and mixed StCsm-RNA-DNA complexes, we performed EMSA analysis of 5'-end radioactively labeled target RNA or DNA by StCsm complexes in the absence of divalent metal ions.

We found that the binary StCsm did not bind a dsDNA 76-mer duplex (Figure S4). On the other hand, it did bind ssDNA oligonucleotides either containing or lacking a protospacer sequence with the same affinity, which, however, was at least ~30-fold lower than the binding of target RNA (Figure S4). Similarly, the StCsm ternary complex, containing target S3/1 RNA, bound ssDNA oligonucleotides irrespective of whether the protospacer sequence was present and with the same affinity as the binary complex. The binding pattern for the binary StCsm complex obtained using the pre-mixed ssDNA/RNA samples nearly overlapped with the binding patterns obtained using individual ssDNA or RNA samples. This finding suggests that the target RNA binding by StCsm does not promote ssDNA binding (and vice versa). Moreover, both ssDNA molecules containing or lacking the protospacer sequence were bound with the same affinity by the ternary StCsm complex. Taken together, our data indicate that StCsm binds RNA and ssDNA molecules independently and that binding occurs at separate sites within the StCsm complex.

Bubbled DNA Degradation by the Ternary StCsm Complex

To test whether single-stranded regions in the context of dsDNA may be targeted by the StCsm ternary complex, we next analyzed cleavage of synthetic DNA duplexes containing unpaired regions of different length (from 1 to 36 nt) that produce DNA bubbles of different size or mismatches. One strand of the bubbled oligoduplex contained a protospacer sequence complementary to the S3 crRNA (S3/1-strand). To monitor cleavage, one of the DNA strands was radioactively labeled, annealed to the complementary strand to form an oligoduplex, mixed with the ternary StCsm complex, supplemented with Mn^{2+} , and aliquots were removed at different intervals. Analysis of the reaction products by denaturing PAGE revealed that the ternary StCsm complex cleaved ssDNA in the bubble/mismatch region on both strands (Figure 2B) depending on the length of the unpaired DNA stretch. Oligoduplexes containing unpaired single-stranded fragments from 12 to 36 nt were cleaved relatively fast, 4–8 nt long were cleaved at a moderate rate, whereas 1–2 nt mismatches were resistant to cleavage (Figure 2C). Notably, the cleavage rate of the strand complementary to crRNA was nearly

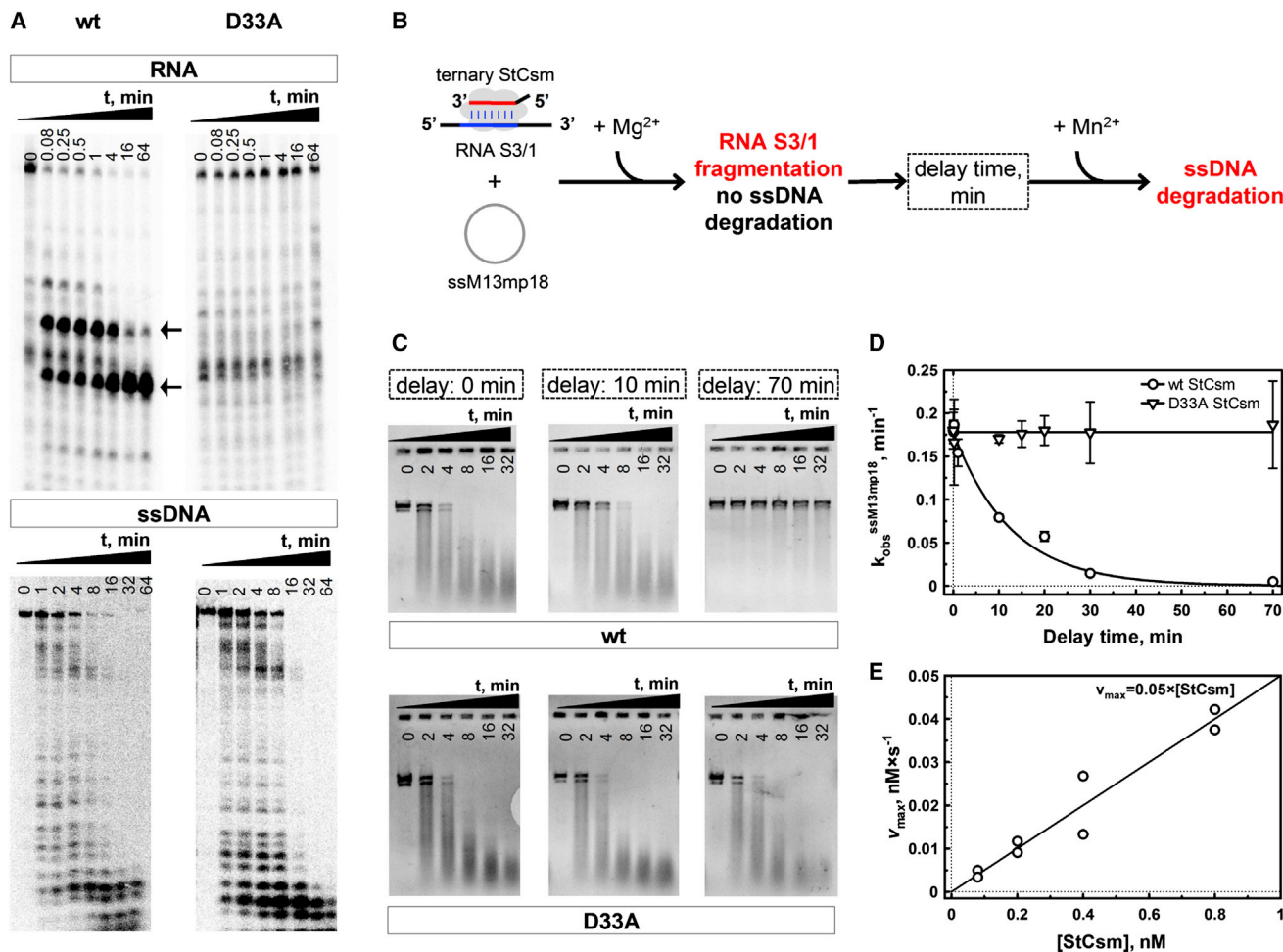


Figure 3. Coupling between RNase and ssDNase Activities of StCsm

(A) RNase and ssDNase activities of wild-type (WT) StCsm and RNA-cleavage deficient StCsm (Csm3 D33A) variant. Cleavage of S3/1 RNA and ssDNA was monitored individually in the reaction mixture containing Mn^{2+} as a cofactor and either ^{33}P -labeled ssDNA or RNA. Reaction conditions were the same as in Figure 2A.

(B) Cartoon depicting the experimental strategy to monitor the temporal control of ssDNase activity of the ternary StCsm. First, StCsm ternary complex is mixed with ssM13mp18 DNA, and RNase cleavage is triggered by addition of Mg^{2+} cofactor. After a certain delay time, the DNase activity is initiated by adding Mn^{2+} .

(C) Representative degradation patterns of ssM13mp18 DNA at three different delay times (0, 10, and 70 min, respectively).

(D) Delay time dependence of degradation rates of ssM13mp18 DNA by the WT StCsm and RNA-cleavage deficient StCsm (Csm3 D33A) variant. DNA degradation rates were determined after the indicated delay times as described in Figure 2.

(E) k_{cat} calculation for RNA hydrolysis by StCsm. Multiple turnover reactions contained 4 nM 5'-labeled RNA S3/1 and 0.08–0.8 nM StCsm.

identical to that of the non-complementary strand (data not shown).

Cleavage Rates of the Activator RNA and ssDNA

Our experimental data indicate that the target RNA binding into the ternary StCsm complex activates ssDNA degradation regardless of whether ssDNA contains a sequence complementary to crRNA. Because Mn^{2+} ions support both RNA (Tamulaitis et al., 2014) and DNA cleavage, we next aimed to establish individual cleavage rates of the activator RNA and ssDNA. To this end, either ssDNA or S3/1 RNA activator molecules were ^{33}P -labeled and subjected to the StCsm digestion followed by analysis of reaction products in the denaturing PAGE. Data analysis revealed that both ssDNA and activator RNA were cleaved in

the StCsm complex; however, two significant differences were observed. First, the RNA cleavage produced fragments of regular size, whereas the DNA cleavage occurred in a random manner. Second, RNA was fragmented much faster than DNA was degraded (Figure 3A). Thus the activator RNA in the StCsm complex was cleaved within 5 s, while the half-time for the ssM13mp18 DNA degradation was ~ 2 min ($k_{obs} = 0.35 \pm 0.07 \text{ min}^{-1}$).

The cleavage rate differences for the activator RNA and ssDNA imply that the RNA cleavage products may remain bound in the StCsm complex and activate ssDNA cleavage. To test this hypothesis, we first pre-incubated the StCsm complex containing the activator S3/1 RNA and the ssM13mp18 DNA in the presence of Mg^{2+} ions, which exclusively support the RNase activity,

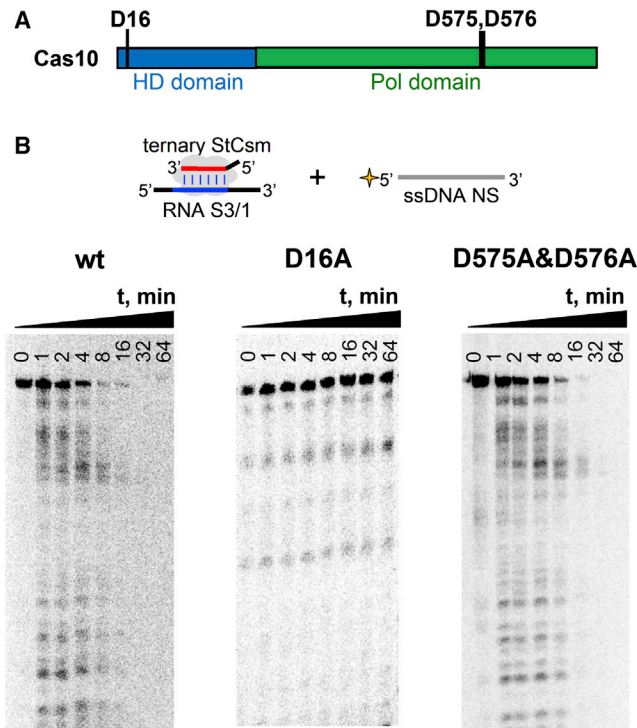


Figure 4. Effect of Cas10 Mutations on the ssDNase Activity of StCsm

(A) Domain architecture of the *S. thermophilus* Cas10 protein. HD-domain denotes HD-type phosphohydrolase/nuclease domain (blue); Pol-domain denotes polymerase/cyclase-like domain (green). Conserved residues characteristic of the different domains and subject to alanine mutagenesis are indicated above the boxes.

(B) ssDNA cleavage by the WT StCsm and StCsm complexes containing Cas10 mutant variants. Reaction components are depicted using the same color scheme as in Figure 1. Cleavage reactions contained 4 nM of ^{33}P -labeled ssDNA NS and 200 nM of ternary StCsm.

and then initiated ssDNA cleavage at different time delays by adding Mn^{2+} , which triggers the DNase activity (Figure 3B). Under these conditions, the activator RNA was cleaved within 5 s; however, the StCsm complex retained ~50% of the ssDNase activity after the 10 min delay from the start of the RNase reaction. We found that after the activator RNA cleavage, the ssDNase activity decreased exponentially with time and became negligible after 70 min (Figures 3C and 3D). The k_{cat} value of $3.0 \pm 0.6 \text{ min}^{-1}$ ($0.05 \pm 0.01 \text{ s}^{-1}$) obtained under a multiple turnover conditions ($[\text{RNA}] > [\text{StCsm}]$) indicates that the release of RNA cleavage products was considerably faster than the decrease of the ssDNase activity (Figure 3E).

To establish whether the activator RNA cleavage is obligatory for ssDNA degradation, we performed cleavage experiments using the StCsm complex containing the RNase-deficient Csm3 D33A mutant (Tamulaitis et al., 2014) (Figure 3A). We found that D33A mutation inhibited RNA cleavage but had no effect on the ssDNA binding and degradation (Figures 3 and S5). Moreover, the RNase-deficient StCsm (Csm3 D33A) variant retained 100% of ssDNase activity even after 70 min preincubation with S3/1 RNA (Figures 3C and 3D), suggesting that in the absence

of the activator RNA cleavage, the StCsm complex is trapped in the ssDNase-active state.

Identification of the DNase Subunit in the StCsm Complex

Cas10 is a signature protein of type III CRISPR-Cas systems and is comprised of a HD-family nuclease and putative polymerase (Pol)/cyclase domains (Figure 4A) (Makarova et al., 2015). In solution *Thermococcus onnurineus* Cas10 protein exhibited a weak ssDNase activity (Jung et al., 2015) that was impaired by the D15N mutation in the HD-domain. In contrast, the DNase activity of the SeCsm complex was compromised by the D586A&D587A mutation in the GGDD-motif of the Cas10 Pol-domain (Samai et al., 2015). To probe whether Cas10 is responsible for the ssDNase activity of the StCsm complex, we analyzed ssDNA cleavage by the wild-type (WT) StCas10 and its mutant variants of the HD- and Pol-domains, respectively. As expected, isolated StCas10 protein exhibited no detectable activity on dsDNA, although basal ssDNase activity on the ssM13mp18 DNA was discernible (Figure S6A). Amino acid residues H15 and D16 in the StCas10 are conserved between Cas10 family members and presumably contribute to the active site in the HD-domain. The D16A replacement in the StCas10 dramatically impaired ssDNA cleavage (Figure S6A). In contrast, the double D575A&D576A mutation of the putative active site in the Pol-domain had no effect on the Cas10 ssDNase activity (Figure S6A). These data suggest that the HD-domain of the Cas10 subunit may be responsible for the ssDNase activity of the StCsm complex.

Indeed, the StCsm complex containing a DNase-deficient Cas10 subunit (D16A) bound both activator RNA S3/1 and ssDNA with the same affinity as the WT StCsm (Figure S6B). Furthermore, the StCsm complex containing Cas10 HD(D16A)- or Pol(D575A&D576A)-domain mutations cleaved activating S3/1 RNA with the same efficiency as the WT ternary StCsm complex (Figure S6C). On the other hand, ssDNA cleavage assay revealed that ssDNase activity of StCsm was impaired by the D16A mutation in the HD-domain whereas the double D575A&D576A mutation in the Pol-domain had no effect on the ssDNase activity of the StCsm complex (Figure 4B).

Identification of Activator RNA Sequence Elements Important for Cas10 DNase Activity

We have shown that the StCsm complex binds and cuts target RNA containing truncations of the protospacer flanking sequence and mismatches in the protospacer (Tamulaitis et al., 2014). Marraffini and Sontheimer demonstrated that protection of the DNA target during conjugation in *S. epidermidis* requires complementarity between fifth and seventh positions in 5'-handle of crRNA and target upstream flanking sequences (Marraffini and Sontheimer, 2010). To test whether changes in the target RNA sequence affect the ssDNase activity of the Csm complex, we analyzed ssM13mp18 DNA cleavage by ternary StCsm complexes pre-loaded with cleavable target RNA molecules containing either truncated 3'- or 5'-flanking sequences, or mismatches (Figure 5). Overall, cleavage analysis revealed that (1) non-complementarity of the S3 spacer 3'-flanking sequence to the 5'-handle of StCsm crRNA promoted

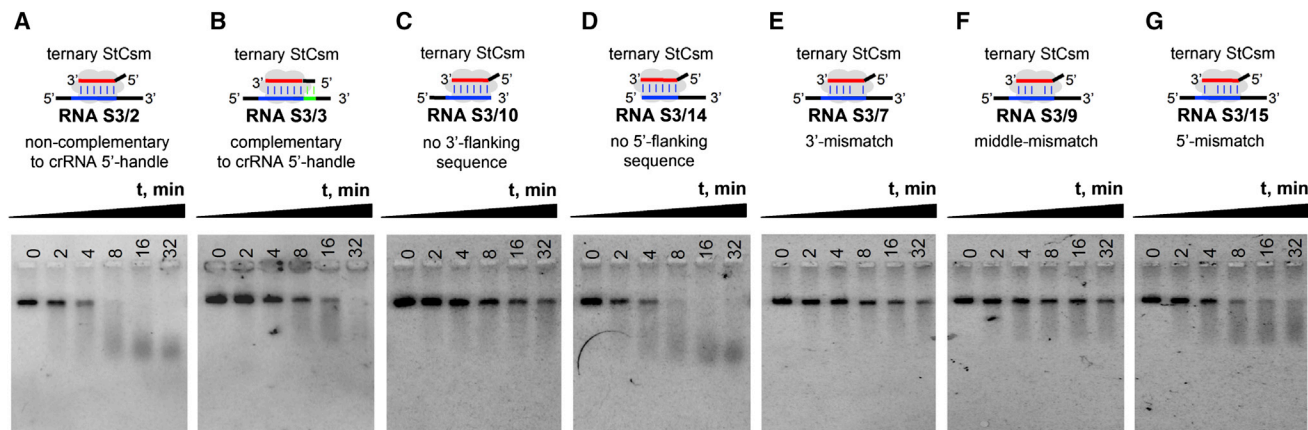


Figure 5. Activator RNA Requirements for the ssDNA Cleavage by the StCsm

(A–G) Cartoons above gels depict ternary StCsm complexes that differ by RNA molecules. The agarose gels show degradation patterns of 1 nM of circular ssDNA M13mp18 in the presence of 5 nM ternary StCsm complexes containing different RNAs (see Figure 1 legend for color coding).

ssM13mp18 DNA degradation (Figure 5A), (2) complementarity between the 3'-flanking sequence and the 5'-handle of the crRNA inhibited ssM13mp18 DNA cleavage (Figure 5B), (3) Watson-Crick base-pairing at positions five to seven was sufficient for inhibition of ssDNA cleavage (Figure S7A), (4) target RNA 3'-flanking (but not 5'-flanking) sequence deletion also inhibited ssM13mp18 DNA cleavage (Figures 5C and 5D), and (5) double mismatches in the target RNA sequence abolished the StCsm ssDNase activity independently of the mismatch position (Figures 5E–5G).

Structural Model of the StCsm Complex

To better understand mechanistic features of the StCsm complex, we constructed its structural model bound to the crRNA-target RNA duplex and ssDNA fragment (Figure 6). Models of individual Csm subunits were based on crystal structures of corresponding Csm and/or Cmr subunits, whereas the entire Csm complex was assembled using a recently determined crystal structure of the Cmr complex (Osawa et al., 2015) as a structural framework. As should be expected from a functionally relevant model, the Csm protein filament closely matches the length of crRNA (40 nt) and the active site aspartates (D33) of Csm3 subunits are positioned in the vicinity of the scissile phosphates of the target RNA (Figure S7B). In the model, the Csm3 filament responsible for the target RNA cleavage and the D16 residue at the active site of the Cas10 HD-domain involved in ssDNA degradation are spatially separated. This raises a question of how target RNA binding/cleavage is coupled to the ssDNA degradation at the HD-nuclease domain of the Cas10 subunit. Although the model is unable to provide the details, it suggests that the complementarity of target RNA with the spacer region of crRNA is monitored by the second filament formed by the Cas10 domain D4 and three copies of a small subunit (Csm2) (Figure S7C) similar to that observed in Cmr and Cascade complexes (Osawa et al., 2015). Conformational changes presumably can propagate through this filament down to the active site at the Cas10 HD-domain. The model does not include the 3'-flanking sequence of the target RNA

because its path through StCsm is unknown. However, it suggests that the exact path of the 3'-flanking sequence will depend on whether the sequence is complementary to the 5'-handle of crRNA. In turn, specific interactions between the 3'-flanking sequence and StCsm may have an allosteric effect on the HD-domain active site.

DISCUSSION

StCsm Functions as Target RNA-Activated Single-Stranded DNase

We have shown that the type III-A StCsm complex guided by crRNA in vitro functions as Me^{2+} -dependent RNase that cleaves ssRNA at five sites regularly spaced by 6 nt intervals (Tamulaitis et al., 2014). Furthermore, in the heterologous *E. coli* strain StCsm restricts ssRNA phage MS2, indicating that in the native host it could be targeting RNA viruses. However, in the *S. thermophilus* type III-A CRISPR array, most of the spacers match DNA phages. This raises a question whether the StCsm complex provides the NA interference exclusively through the phage RNA cleavage or invading DNA is also targeted and destroyed. To address this question, we chose a biochemical approach combined with structural modeling.

Consistent with previous studies we have shown that the binary StCsm complex in vitro neither binds nor cuts dsDNA (Figures S1 and S4), although it slowly degrades linear or circular ssDNA (Figures 1 and 2A). Target RNA binding by the binary StCsm has no effect on the dsDNA cleavage (Figure S1); however, it significantly (~ 10 -fold) stimulates ssDNA degradation regardless of the DNA sequence: DNA containing a protospacer matching crRNA is degraded at the same rate as any other DNA (Figures 1B and 1C). In the ternary StCsm complex bound to the ssDNA, the target RNA is cleaved simultaneously with ssDNA albeit at a much faster rate (Figure 3A). Surprisingly, the RNA cleavage is not required for the activation of the ssDNase: the RNA-cleavage deficient StCsm (Csm3 D33A) complex stimulates ssDNA cleavage as a cleavage-proficient WT StCsm complex (Figure 3). Taken together, these experiments indicate that

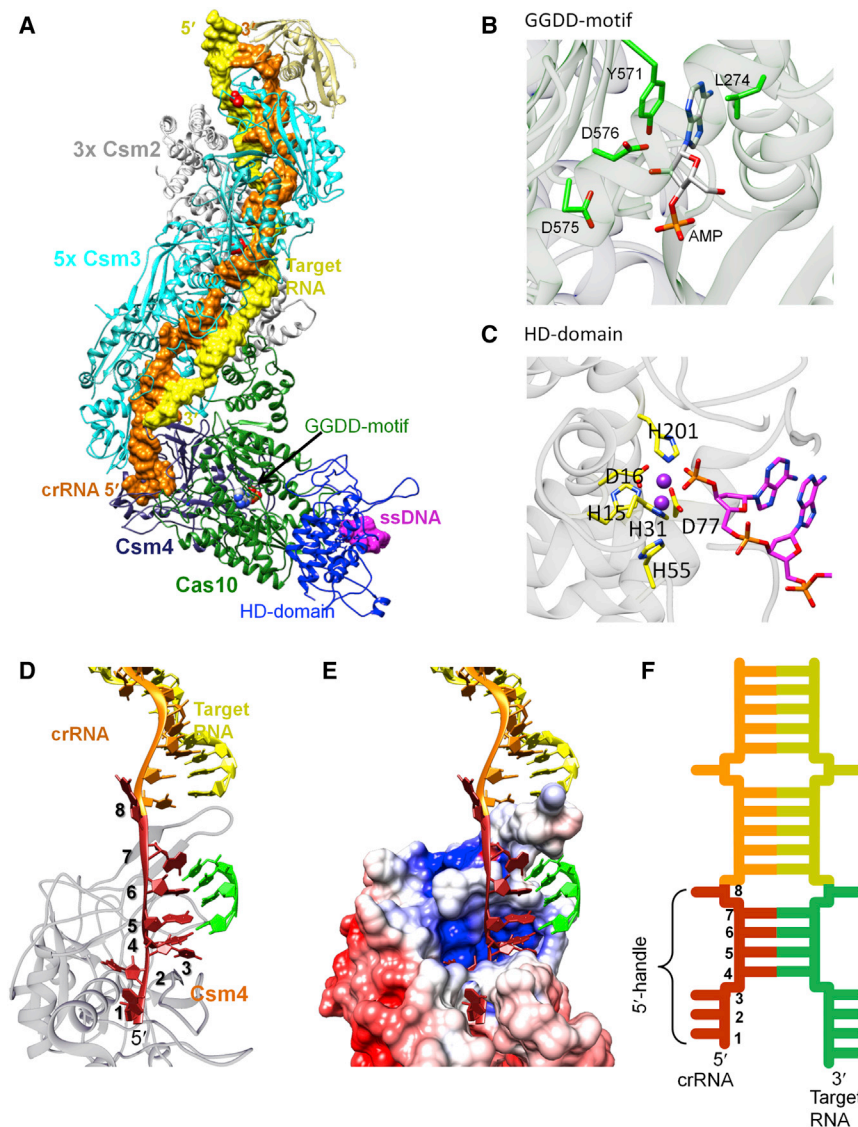


Figure 6. Structural Arrangement of the StCsm Complex

(A) 3D model of the StCsm complex (Csm1-5). crRNA and target RNA are shown with their surface shown as orange and yellow, respectively. ssDNA bound to the active site of the HD-domain is shown in pink. Csm subunits appear in different colors. Side chains of the Csm3 active site residues (D33) are shown in red.

(B) The nucleotide-binding site in the GGDD-domain. Residues contributing to the nucleotide binding are shown with their side chains.

(C) The active site of the HD-domain of Cas10 complexed with ssDNA fragment. Side chains of residues involved in coordination of two metal ions (magenta balls) are shown in yellow.

(D) crRNA bound to Csm4. crRNA 5'-handle is depicted red, green shows a complementary RNA fragment that could bind to the 4–7 nt of crRNA ensuring self versus non-self discrimination.

(E) Same as in (D), with depicted molecular surface of the Csm4 model colored according to electrostatic potential (blue, positive; red, negative).

(F) A schematic representation of self target RNA recognition by crRNA. RNA colors and nucleotide numbers are the same as those in (D) and (E).

StCsm functions as a non-specific ssDNase that is activated by the target RNA (Figure 7A).

In StCsm, the Csm3 subunit acts as a RNase that cuts target RNA but not DNA (Tamulaitis et al., 2014). This raises a question about the localization of the DNase active site in StCsm. The Cas10 protein contains an N-terminal HD-domain and a Pol-domain (Makarova et al., 2015). Ramia et al. demonstrated that an isolated Csm1 (Cas10) protein of the *Staphylococcus epidermidis* (SeCsm1) cleaves ssDNA and although the GGDD motif is directly responsible for this 3' to 5' exonuclease activity, the HD-domain takes part in this process (Ramia et al., 2014b). Conversely, in *T. onnurineus*, the stand-alone Cas10 protein exhibited a weak ssDNase activity that was impaired by mutation in the HD-domain (Jung et al., 2015). HD-domain was also responsible for the ssDNA cleavage by the Cas3 nuclease/helicase of the type I CRISPR-Cas system (Sinkunas et al., 2011). Contrary to Ramia et al., Marraffini and coworkers had shown that mutations in the Pol-domain (containing GGDD

motif) but not in the HD-domain of the SeCsm1 prevented CRISPR-Cas immunity of *Staphylococcus epidermidis* (Hattoum-Aslan et al., 2014). Furthermore, D586A&D587A mutation in the GGDD-site of Pol-domain compromised DNase activity of the SeCsm (Samai et al., 2015). This prompted us to investigate whether the StCas10 HD- or Pol-domain is responsible for the ssDNA degradation by the StCsm complex. We found that D16A mutation in the HD-domain of StCas10 abolished ssDNase activity of the StCsm complex (Figure 4), whereas alanine mutations of the conserved aspartate residues D575 and D576 in the GGDD-motif of the Cas10 subunit had no effect on the ssDNase activity. Collectively, these data indicate that the StCsm complex degrades ssDNA in a target RNA-dependent manner using the active site within the HD-domain of the Cas10 subunit (Figures 6 and 7A). Experimental conditions differ between the assay used here and transcription-dependent assay (Samai et al., 2015) where NTPs and RNA polymerase were present in the reaction mixture together with template DNA. The molecular details of role of Pol-domain in the immunity provided by the type III-A system of *S. thermophilus* remain to be established.

Coupling between the Target RNA Binding and DNA Degradation

In the binary StCsm complex, Cas10 manifests weak ssDNA degradation activity, which is, however, increased dramatically upon binding of the activator (target) RNA (Figure 1). This raises a question on the coupling mechanism between the activator

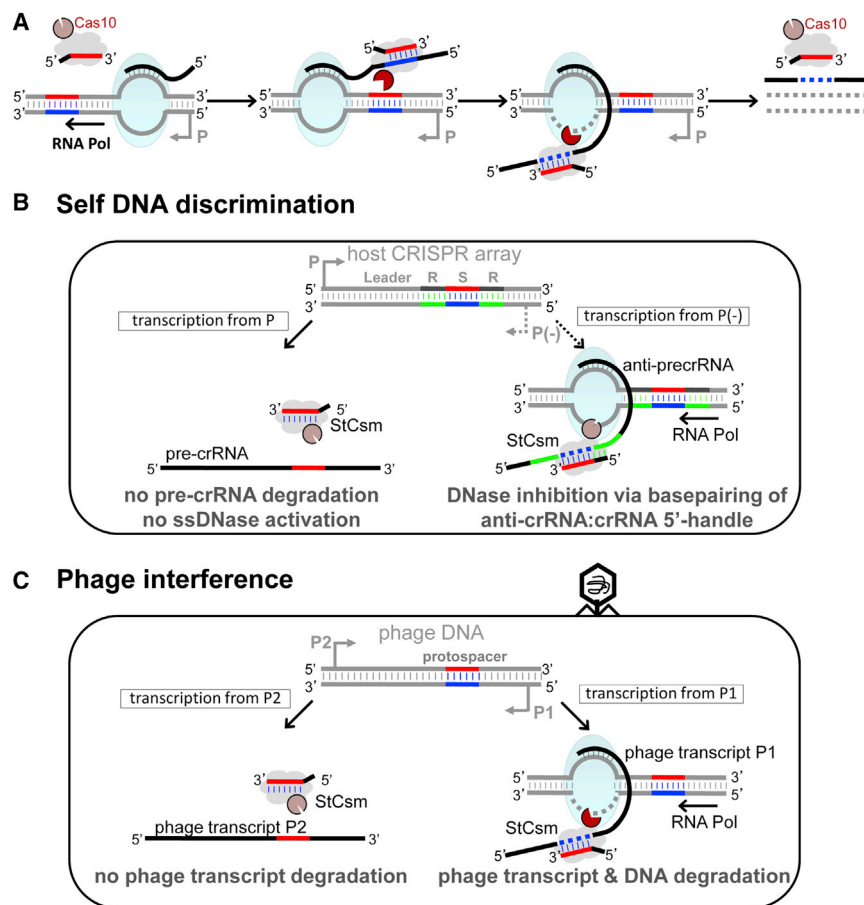


Figure 7. Mechanisms of Immunity Provided by the Type III-A CRISPR-Cas System

(A) Possible in vivo mechanism for NA interference by the type III-A Csm complex. When foreign DNA enters the cell, transcription is initiated to establish the phage infection. If transcription occurs through the region containing a protospacer, the nascent phage mRNA emerging from the transcription complex becomes a target for the StCsm complex. RNA transcript binding by StCsm complex activates Cas10 protein for in cis degradation of the non-template ssDNA emerging from the transcription bubble. Subsequent target RNA degradation represses ssDNase activity of the StCsm.

(B) Self-DNA discrimination by the type III system of *S. thermophilus*. Pre-crRNA transcribed from P promoter on the template strand of host CRISPR array does not bind crRNA and therefore will not activate Cas10 ssDNase. In case of bidirectional transcription through the CRISPR array, anti-precrRNA transcribed from a putative promoter P(-) on the non-template strand will bind to the StCsm-complex due to complementarity to crRNA. However, complementarity between the crRNA 5'-handle and 3'-flanking sequence will repress ssDNase activity protecting host DNA from cleavage.

(C) Non-self DNA degradation by the type III system of *S. thermophilus*. In case of phage infection RNA transcribed from the P1 promoter on the template strand crRNA will base-pair to the spacer region but not to the 5'-handle of Csm complex, and therefore will activate phage DNA degradation by the Cas10 ssDNase. In case of phage RNA transcription from the putative promoter on the non-template strand, resulting RNA will be resistant to cleavage by the Csm complex.

RNA binding/cleavage and DNA degradation by the Cas10 protein. The backbone of the Csm complex is composed of a 5xCsm3 protein filament that is capped by the Cas10-Csm4 subcomplex at one end and by the Csm5 subunit at the opposite end (Figure 6). The 5'-handle of crRNA is presumably bound by the Csm4 subunit, whereas Csm3 protein filament provides a padlock for binding of the crRNA spacer region that is engaged in base-pairing interactions with the target RNA. Because our StCsm model does not allow to unambiguously predict Csm protein subunits/residues that might be involved in signal transmission between the target RNA binding and DNA hydrolysis, we investigated the target RNA requirements for the activation of the ssDNA cleavage by the HD-domain of Cas10 protein (Figure 5). We have found that 5'-end truncations of the target RNA have no effect on the ssDNA cleavage. Surprisingly, the 3'-end truncations of the target RNA completely abolished ssDNA cleavage. Importantly, both the 5'- and 3'-end truncated target RNA molecules are cleaved by the Csm complex into 6 nt products (Tamulaitis et al., 2014). This finding indicates that the 3'-end of target RNA plays an important role in coupling between the target RNA binding and DNA cleavage at the HD-domain of the Cas10 protein.

Autoimmunity Problem in Type III CRISPR-Cas Systems

The CRISPR-Cas system in prokaryotes and archaea functions as an acquired immune system that must destroy invading

foreign nucleic acids but prevent targeting host's own DNA. In the DNA-targeting type I and II systems, PAM sequence plays a key role in discrimination between self and non-self DNA by licensing crRNA-guided base-pairing to the protospacer sequence and subsequent cleavage (Sternberg et al., 2014; Szczelkun et al., 2014). Because PAM is absent near the protospacer in the CRISPR array, host DNA is resistant to cleavage whereas foreign DNA (e.g., viral DNA), bearing protospacers flanked by PAM, is degraded.

Effector complexes of type III-A and III-B systems cleave RNA in a PAM-independent manner. In theory, if RNA is the targeted nucleic acid in the cell, the autoimmunity problem does not arise. First, crRNA generated by maturation of the pre-crRNA transcribed from the CRISPR array will be unable to base-pair to its own precursor. Second, even if the type III system would target host RNA, e.g., resulting from the antisense transcription of CRISPR array, host DNA will remain intact (Figure 7B).

However, in vivo type III-A SeCsm complex also targets DNA in a transcription-dependent manner (Samai et al., 2015), and this raises a question how self versus non-self DNA is discriminated in this case. Complementarity between the 5'-handle of the crRNA and the target DNA plays a key role in self versus non-self discrimination: 5'-handle matching the DNA sequence flanking the protospacer, permits DNA conjugation, whereas non-complementary 5'-handle restricts DNA transfer (Maraffini

and Sontheimer, 2010). The 5'-handle of crRNA originates from the repeat and therefore is inevitably complementary to the repeat fragment in the CRISPR array. The protospacer in the viral DNA will usually be flanked by a sequence non-complementary to the 5'-handle and such DNA will be degraded. This model is supported by in vivo studies; however, it has been never proven by biochemical experiments.

The Complementarity of the 5'-Handle of crRNA to the Target RNA but Not DNA Protects Host DNA from Degradation

Using closed circular ssDNA as a model substrate, we demonstrate here that complementarity/non-complementarity of the 5'-handle of crRNA to the 3'-flanking sequence of the DNA have no effect on the DNA cleavage pattern: both DNA molecules are degraded at the same rate regardless of the 3'-flanking sequence (Figure 1). On the other hand, we convincingly show that the complementarity/non-complementarity of the 5'-handle of crRNA to the 3'-flanking sequence of the target RNA is critical for the ssDNase activity of Cas10 HD-domain (Figure 5). Indeed, StCsm binary complex binding to the RNA target through base-pairing interactions with crRNA activates ssDNA degradation only if 3'-flanking sequence of the target RNA is non-complementary to 5'-handle of crRNA. If 3'-flanking sequence of the target RNA is complementary to 5'-handle of crRNA, DNA degradation is repressed.

Such a mechanism should allow discrimination of self versus non-self DNA during transcription-dependent DNA cleavage. Pre-crRNA transcribed from the template strand of CRISPR array will not bind crRNA and therefore will not trigger host DNA degradation (Figure 7B). The problem of autoimmunity will arise if a non-template strand is transcribed. In this case, antisense RNA transcribed through the CRISPR array will match the crRNA and may activate host DNA cleavage by the Csm complex (Figure 7B). Antisense transcription is quite widespread in bacteria and plays a role in mRNA processing (Lasa et al., 2011). Moreover, in *S. sulfolobus*, the type III-B CRISPR array is transcribed in both directions, producing antisense crRNAs (Lillestøl et al., 2009). However, if antisense RNA is produced from the CRISPR array, it will be complementary both to the spacer region and to the 5'-handle of crRNA. We have shown previously that the complementarity of target RNA to the 5'-handle of crRNA did not prevent RNA cleavage (Tamulaitis et al., 2014); however, we demonstrate here that it represses DNA degradation. The hypothesis proposed from biochemical experiments is supported by the structural model of the StCsm complex. Indeed, as the spacer region of crRNA is base-paired with the target RNA, it is easy to envision base-pairing extending into the 5'-handle of crRNA. Our molecular model of the Csm complex offers a number of structural insights into such base-pairing. The crRNA 5'-handle consists of 8 nt that are bound by Csm4. However, the Csm model predicts that not all positions of the handle are accessible for Watson-Crick pairing. The first 3 nt are embedded into distinct pockets of Csm4 whereas the eighth nt, similar to every sixth position in the spacer region of crRNA, is flipped out by the thumb of Csm4 (Figure 6F). Only nucleobases in positions four to seven form a quadruple helical stack similar to the A-form RNA and are readily available for

base-pairing. It turns out that these structure-based predictions are fully supported by our in vitro experiments reported here and in vivo experiments performed with a related Csm complex from *S. epidermidis* (Marraffini and Sontheimer, 2010). Our biochemical experiments show that the complementarity at the handle positions four to seven protects ssDNA from degradation similarly as the full complementarity, whereas the complementarity at the positions one to three and eight offers no protection at all (Figure S7A). Even three Watson-Crick base-pairs at positions five to seven significantly inhibit the ssDNase activity (Figure S7A). These results are in good agreement with the *S. epidermidis* in vivo experiments showing that the complementarity at the same three positions (fifth to seventh) of the crRNA 5'-handle is important for protection of self DNA (Marraffini and Sontheimer, 2010). Combined with our model, these experiments strongly suggest that the complementarity test involves only the three or four positions of the crRNA 5'-handle and does not result in significant conformational changes of either the crRNA handle or Csm4. Instead, it appears likely that the presence or absence of the base-pairing with the crRNA 5'-handle directs the target RNA by two different paths on the surface of Cas10. Presumably, only the RNA following one of these paths (not involved in pairing with the 5'-handle) through allosteric modulation is able to activate HD-domain. This idea is consistent with our experimental data showing that not only the complementarity with the crRNA 5'-handle but also the absence of the 3'-flanking sequence of the target RNA protects ssDNA from degradation (Figures 5B and 5C). A similar crRNA-target RNA complementarity check has been recently reported for type III-B Cmr complexes (Elmore et al., 2016; Estrella et al., 2016).

Spatiotemporal Regulation of the Target RNA-Coupled DNA Degradation by the Csm Complex

Taken together, data provided here are consistent with the following model for nucleic acid interference by the type III-A Csm complex (Figure 7). When foreign DNA, for example phage DNA, enters the cell, transcription is initiated to establish phage infection. If transcription occurs through the region containing a protospacer, the nascent phage mRNA emerging from the transcription complex becomes a target for the Csm complex. crRNA binding through base-pairing to the complementary sequence in nascent mRNA will tether the Csm complex to the transcribed DNA and activate Cas10 protein for in cis degradation of the ssDNA emerging from the transcription bubble (Figures 7, S7D, and S7E). This will couple DNA cleavage to the transcription of specific mRNA that contains crRNA matching sequence and limit DNase activity to the phage DNA. StCsm reactions on DNA bubbles (Figures 2B and 2C) show that unpaired DNA regions of 12–36 nt are effectively targeted by the StCsm complex. In the transcription elongation complex ~18 bp of DNA are melted and therefore could be potentially targeted by the StCsm complex (Barnes et al., 2015; Zuo and Steitz, 2015). The upstream portion of the non-template strand appears to lie on the surface of RNA polymerase with the bases exposed, based on its accessibility to nucleases and hydroxyl radical (Wang and Landick, 1997). Taken together, these data are in good agreement with the transcription-dependent DNA

cleavage pattern of SeCsm (Samai et al., 2015), which shows DNA cleavage of only the non-template strand.

In theory, RNA-activated Csm complex could cleave in *trans* any ssDNA in the host cell, for example, single-stranded DNA replication intermediates, and cause damage to the host genome. Such “off-target” ssDNA cleavage would require that the Csm complex remain in the activated RNA-bound state for a certain time. In fact, the activating RNA bound to StCsm is cleaved rapidly (in scale of seconds) into 6 nt products that are released into solution. Pre-incubation of the RNA-loaded Csm complex with Mg²⁺ that triggers RNA (but not DNA) cleavage results in a gradual decrease of the DNase activity suggesting that the dissociation of reaction products represses the ssDNA cleavage activity of the Csm complex (Figures 3B–3D).

Thus, tethering of StCsm complex to the transcript confines DNase activity within a limited space near nascent mRNA while fast RNA degradation ensures a temporal regulation of DNase activity avoiding the potential cleavage of the host genome. A similar mechanism enables RNA-directed DNA methylation in plants (Movahedi et al., 2015), where small 24 nt siRNAs bound to Ago4 protein direct molecular machinery that catalyzes heterochromatic histone modifications or DNA methylation to specific genome loci by base-pairing with long non-coding RNAs that are associated with the chromatin. In the case of type III-A CRISPR-Cas systems, the RNA transcript can act as a tether that attaches StCsm complex through crRNA-RNA interactions to a specific location in the genome and recruits Cas10 nuclease to DNA. Transcript RNA binding activates Cas10 DNase for DNA cleavage in *cis*, whereas subsequent RNA cleavage by the Csm3 subunit in the Csm complex provides a temporal control by suppressing DNase activity to prevent in *trans* action that could result in the host genome damage. This provides an efficient fail-safe mechanism for degradation of phage mRNA and transcriptionally coupled DNA meanwhile maintaining host genome integrity. On the other hand, the ease of reprogramming the Csm complex with different crRNAs paves the way for the development of novel molecular tools for the selective targeting of mRNA and actively transcribed DNA.

EXPERIMENTAL PROCEDURES

Experimental procedures are described in detail in the [Supplemental Experimental Procedures](#). Point mutations in *cas10* and *csm3* genes were introduced using Quick Change Mutagenesis. WT and mutant StCsm complexes were obtained as described previously (Tamulaitis et al., 2014). Details on nucleic acids used in this study, DNA, and RNA binding and cleavage assays are provided in [Table S1](#) and in the [Supplemental Experimental Procedures](#). A structural model of the StCsm complex was obtained using template-based modeling approach.

SUPPLEMENTAL INFORMATION

Supplemental Information includes Supplemental Experimental Procedures, seven figures, and one table and can be found with this article online at <http://dx.doi.org/10.1016/j.molcel.2016.03.024>.

AUTHOR CONTRIBUTIONS

M.K., G.T., and V.S. designed research; M.K., G.T., and G.K. performed research; Č.V. performed modeling experiments; M.K., G.T., Č.V., and V.S.

analyzed data; and G.T., Č.V., and V.S. wrote the paper. All authors read and approved the final manuscript.

ACKNOWLEDGMENTS

We thank Mantvyda M. Grusyte for help with plasmids construction. We also thank Dr. Philippe Horvath (DuPont) for discussions. The work in part has been supported by the Research Council of Lithuania (grant MIP-40/2013 to G.T.). Publication of this article was funded by the Research Council of Lithuania.

Received: December 29, 2015

Revised: February 25, 2016

Accepted: March 22, 2016

Published: April 21, 2016

REFERENCES

- Barnes, C.O., Calero, M., Malik, I., Graham, B.W., Spahr, H., Lin, G., Cohen, A.E., Brown, I.S., Zhang, Q., Pullara, F., et al. (2015). Crystal structure of a transcribing RNA polymerase II complex reveals a complete transcription bubble. *Mol. Cell* 59, 258–269.
- Benda, C., Ebert, J., Scheltema, R.A., Schiller, H.B., Baumgärtner, M., Bonneau, F., Mann, M., and Conti, E. (2014). Structural model of a CRISPR RNA-silencing complex reveals the RNA-target cleavage activity in Cmr4. *Mol. Cell* 56, 43–54.
- Deng, L., Garrett, R.A., Shah, S.A., Peng, X., and She, Q. (2013). A novel interference mechanism by a type IIIB CRISPR-Cmr module in *Sulfolobus*. *Mol. Microbiol.* 87, 1088–1099.
- Elmore, J.R., Sheppard, N.F., Ramia, N., Deighan, T., Li, H., Terns, R.M., and Terns, M.P. (2016). Bipartite recognition of target RNAs activates DNA cleavage by the type III-B CRISPR-Cas system. *Genes Dev.* 30, 447–459.
- Estrella, M.A., Kuo, F.T., and Bailey, S. (2016). RNA-activated DNA cleavage by the type III-B CRISPR-Cas effector complex. *Genes Dev.* 30, 460–470.
- Gasiunas, G., Barrangou, R., Horvath, P., and Siksnys, V. (2012). Cas9-crRNA ribonucleoprotein complex mediates specific DNA cleavage for adaptive immunity in bacteria. *Proc. Natl. Acad. Sci. USA* 109, E2579–E2586.
- Gasiunas, G., Sinkunas, T., and Siksnys, V. (2014). Molecular mechanisms of CRISPR-mediated microbial immunity. *Cell. Mol. Life Sci.* 71, 449–465.
- Goldberg, G.W., Jiang, W., Bikard, D., and Marraffini, L.A. (2014). Conditional tolerance of temperate phages via transcription-dependent CRISPR-Cas targeting. *Nature* 514, 633–637.
- Hale, C.R., Cocozaki, A., Li, H., Terns, R.M., and Terns, M.P. (2014). Target RNA capture and cleavage by the Cmr type III-B CRISPR-Cas effector complex. *Genes Dev.* 28, 2432–2443.
- Hatoum-Aslan, A., Maniv, I., Samai, P., and Marraffini, L.A. (2014). Genetic characterization of antiplasmid immunity through a type III-A CRISPR-Cas system. *J. Bacteriol.* 196, 310–317.
- Jackson, R.N., Golden, S.M., van Erp, P.B., Carter, J., Westra, E.R., Brouns, S.J., van der Oost, J., Terwilliger, T.C., Read, R.J., and Wiedenheft, B. (2014). Structural biology. Crystal structure of the CRISPR RNA-guided surveillance complex from *Escherichia coli*. *Science* 345, 1473–1479.
- Jinek, M., Chylinski, K., Fonfara, I., Hauer, M., Doudna, J.A., and Charpentier, E. (2012). A programmable dual-RNA-guided DNA endonuclease in adaptive bacterial immunity. *Science* 337, 816–821.
- Jung, T.Y., An, Y., Park, K.H., Lee, M.H., Oh, B.H., and Woo, E. (2015). Crystal structure of the Csm1 subunit of the Csm complex and its single-stranded DNA-specific nuclease activity. *Structure* 23, 782–790.
- Lasa, I., Toledo-Arana, A., Dobin, A., Villanueva, M., de los Mozos, I.R., Vergara-Irigaray, M., Segura, V., Fagegaltier, D., Penadés, J.R., Valle, J., et al. (2011). Genome-wide antisense transcription drives mRNA processing in bacteria. *Proc. Natl. Acad. Sci. USA* 108, 20172–20177.
- Lillestøl, R.K., Shah, S.A., Brügger, K., Redder, P., Phan, H., Christiansen, J., and Garrett, R.A. (2009). CRISPR families of the crenarchaeal genus

- Sulfolobus: bidirectional transcription and dynamic properties. *Mol. Microbiol.* **72**, 259–272.
- Makarova, K.S., Wolf, Y.I., Alkhnbashi, O.S., Costa, F., Shah, S.A., Saunders, S.J., Barrangou, R., Brouns, S.J., Charpentier, E., Haft, D.H., et al. (2015). An updated evolutionary classification of CRISPR-Cas systems. *Nat. Rev. Microbiol.* **13**, 722–736.
- Marraffini, L.A., and Sontheimer, E.J. (2008). CRISPR interference limits horizontal gene transfer in staphylococci by targeting DNA. *Science* **322**, 1843–1845.
- Marraffini, L.A., and Sontheimer, E.J. (2010). Self versus non-self discrimination during CRISPR RNA-directed immunity. *Nature* **463**, 568–571.
- Movahedi, A., Sun, W., Zhang, J., Wu, X., Mousavi, M., Mohammadi, K., Yin, T., and Zhuge, Q. (2015). RNA-directed DNA methylation in plants. *Plant Cell Rep.* **34**, 1857–1862.
- Mulepati, S., Héroux, A., and Bailey, S. (2014). Structural biology. Crystal structure of a CRISPR RNA-guided surveillance complex bound to a ssDNA target. *Science* **345**, 1479–1484.
- Osawa, T., Inanaga, H., Sato, C., and Numata, T. (2015). Crystal structure of the CRISPR-Cas RNA silencing Cmr complex bound to a target analog. *Mol. Cell* **58**, 418–430.
- Peng, W., Feng, M., Feng, X., Liang, Y.X., and She, Q. (2015). An archaeal CRISPR type III-B system exhibiting distinctive RNA targeting features and mediating dual RNA and DNA interference. *Nucleic Acids Res.* **43**, 406–417.
- Ramia, N.F., Spilman, M., Tang, L., Shao, Y., Elmore, J., Hale, C., Cocozaki, A., Bhattacharya, N., Terns, R.M., Terns, M.P., et al. (2014a). Essential structural and functional roles of the Cmr4 subunit in RNA cleavage by the Cmr CRISPR-Cas complex. *Cell Rep.* **9**, 1610–1617.
- Ramia, N.F., Tang, L., Cocozaki, A.I., and Li, H. (2014b). Staphylococcus epidermidis Csm1 is a 3′-5′ exonuclease. *Nucleic Acids Res.* **42**, 1129–1138.
- Samai, P., Pyenson, N., Jiang, W., Goldberg, G.W., Hatoum-Aslan, A., and Marraffini, L.A. (2015). Co-transcriptional DNA and RNA cleavage during type III CRISPR-Cas immunity. *Cell* **161**, 1164–1174.
- Sinkunas, T., Gasiunas, G., Fremaux, C., Barrangou, R., Horvath, P., and Siksnys, V. (2011). Cas3 is a single-stranded DNA nuclease and ATP-dependent helicase in the CRISPR/Cas immune system. *EMBO J.* **30**, 1335–1342.
- Staals, R.H., Agari, Y., Maki-Yonekura, S., Zhu, Y., Taylor, D.W., van Duijn, E., Barendregt, A., Vlot, M., Koehorst, J.J., Sakamoto, K., et al. (2013). Structure and activity of the RNA-targeting type III-B CRISPR-Cas complex of *Thermus thermophilus*. *Mol. Cell* **52**, 135–145.
- Sternberg, S.H., Redding, S., Jinek, M., Greene, E.C., and Doudna, J.A. (2014). DNA interrogation by the CRISPR RNA-guided endonuclease Cas9. *Nature* **507**, 62–67.
- Szczelkun, M.D., Tikhomirova, M.S., Sinkunas, T., Gasiunas, G., Karvelis, T., Pschera, P., Siksnys, V., and Seidel, R. (2014). Direct observation of R-loop formation by single RNA-guided Cas9 and Cascade effector complexes. *Proc. Natl. Acad. Sci. USA* **111**, 9798–9803.
- Tamulaitis, G., Kazlauskienė, M., Manakova, E., Venclovas, Č., Nwokeoji, A.O., Dickman, M.J., Horvath, P., and Siksnys, V. (2014). Programmable RNA shredding by the type III-A CRISPR-Cas system of *Streptococcus thermophilus*. *Mol. Cell* **56**, 506–517.
- Wang, D., and Landick, R. (1997). Nuclease cleavage of the upstream half of the nontemplate strand DNA in an *Escherichia coli* transcription elongation complex causes upstream translocation and transcriptional arrest. *J. Biol. Chem.* **272**, 5989–5994.
- Westra, E.R., van Erp, P.B., Künne, T., Wong, S.P., Staals, R.H., Seegers, C.L., Bollen, S., Jore, M.M., Semenova, E., Severinov, K., et al. (2012). CRISPR immunity relies on the consecutive binding and degradation of negatively supercoiled invader DNA by Cascade and Cas3. *Mol. Cell* **46**, 595–605.
- Zhang, J., Rouillon, C., Kerou, M., Reeks, J., Brugger, K., Graham, S., Reimann, J., Cannone, G., Liu, H., Albers, S.V., et al. (2012). Structure and mechanism of the CMR complex for CRISPR-mediated antiviral immunity. *Mol. Cell* **45**, 303–313.
- Zhao, H., Sheng, G., Wang, J., Wang, M., Bunkoczi, G., Gong, W., Wei, Z., and Wang, Y. (2014). Crystal structure of the RNA-guided immune surveillance Cascade complex in *Escherichia coli*. *Nature* **515**, 147–150.
- Zhu, X., and Ye, K. (2015). Cmr4 is the slicer in the RNA-targeting Cmr CRISPR complex. *Nucleic Acids Res.* **43**, 1257–1267.
- Zuo, Y., and Steitz, T.A. (2015). Crystal structures of the *E. coli* transcription initiation complexes with a complete bubble. *Mol. Cell* **58**, 534–540.